Progress in Physics of Applied Materials 7 (2027), Serial Number 14, 37-48

Semnan University

Progress in Physics of Applied Materials

journal homepage: https://ppam.semnan.ac.ir/

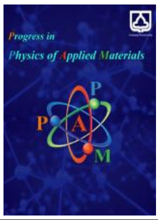


# Faraday Effect for Magnetic Sensitivity Measurement in Different Types of Optical Fibers

**Suha Mousa Khorsheed *, Roaa T. Abdulla, Zeena M. Al-Azzawi, Wasan A. Al-Dulaimi**

*Department of Physics, College of Science, Al-Nahrain University, Baghdad, Iraq*

**ARTICLE INFO**

Article history:
Received: 20 May 2026
Revised: 20 June 2026
Accepted: 26 June 2026
Published online: 1 August 2026

Keywords:
Optical fibers;
Fiber Bragg grating;
Verdet constant;
Magnetic sensors.

**ABSTRACT**

This research explores the Faraday effect in optical fibers and its exploitation to enhance the sensitivity of magnetic field measurements using fiber Bragg grating technology. The aim is to develop a more efficient magnetic sensor by modifying the traditional Faraday experiment and replacing the conventional optical fiber with a multi-grid Bragg fiber. A modified experimental setup was designed using an infrared laser and Bragg fibers with varying numbers of gratings (from one to four regions), and the effect of current intensity and spacing between the electrodes on the magnetic field strength was investigated. The results showed that the magnetic field increases linearly with the current, and the optimal field distribution is achieved at an average spacing between the coils. Furthermore, the results indicated that increasing the number of gratings leads to increased sensitivity due to the amplification of the Faraday effect and the extension of the effective length of the optical interaction. The four-segmented fiber exhibited a sensitivity of 93 $w/T$ higher than the conventional fiber, although an optimal limit to the number of gratings was noted, as excessive grating leads to signal loss and response saturation. It has been observed that the change in magnetic response depends primarily on polarization rotation rather than wavelength shift, due to the small value of the Verdet constant in silica at a wavelength of 1550 nm. This has made the use of multi-segment Bragg fibers an effective approach for improving the performance of magneto-optical sensors, with the potential for development into high-precision electromagnetic measurement applications.

## 1. Introduction

Optical fibers are fundamental technologies in advanced communications and signal and data transmission, this makes transmitting massive amounts of data of minimal signal loss and high speeds over long distances. Among current applications in optical fibers, the Faraday effect in magnetic fields is a crucial phenomenon, significantly impacting the quality of optical fibers. The Faraday effect involves the interaction of light with the magnetic field passing through the optical fiber, resulting in a change in the polarization of the passing light [1]. This allows the use of fiber Bragg grating (FBG) technology to accurately sense electric current without subjecting the fiber to mechanical stress by measuring changes in the wavelength reflected from the FBG. This method enhances the ability to use this technology for highly accurate and focused sensing of magnetic and electric fields. Because the Faraday effect is wavelength-dependent only, it is well-suited for magnetic field sensing applications using silica glass optical fibers [2].

In FBGs, the stress caused by magnetic fields on metal bases supporting the optical fiber causes a change in wavelength. This approach allows for the indirect calculation of magnetic field strength, making it a viable alternative to conventional techniques in sensitive

* Corresponding author.
*E-mail address:* suha.korsheed@nahrainuniv.edu.iq

**Cite this article as:**

Khorsheed, S.M., Abdulla, R.T., Al-Azzawi, Z.M. and Al-Dulaimi, W.A., 2027. Faraday Effect for Magnetic Sensitivity Measurement in Different Types of Optical Fibers. *Progress in Physics of Applied Materials*, *7*(1) pp.37-48.
DOI: **10.22075/ppam.2026.41285.1230**

applications, as illustrated in Figure 1 [3]. Furthermore, doping silica fibers with gadolinium ions amplifies the Faraday effect, doubling its effect compared to conventional fibers, thus promoting the development of more efficient optical dielectrics for optical communication systems [4]. This impacts the efficiency of optical sensors such as fiber gyroscopes, which utilize PM-PBF fibers that are less affected than conventional fibers, making them a suitable option for sensitive applications [5]. The following is a detailed mathematical description of the Bragg diffraction grating and how to calculate the Verdet constant, which is used to sense changes in the magnetic field occurring in the optical fiber opposite the Bragg diffraction grating.

### 1.1. Fiber Bragg Gratings

Fiber Bragg gratings are fabricated by exploiting the light sensitivity of the fiber core using interfering ultraviolet beams. This process is governed by optical parameters such as light intensity and interference angle, which control the modulation of the periodic refractive index and allow for precise tuning of the grating's spectral reflectance characteristics [6,7]. FBG sensors are characterized by high sensitivity and resistance to electromagnetic interference, but they face challenges such as the interplay between temperature and stress sensitivity. Their crucial role is highlighted in detecting the Faraday effect in the presence of magnetic fields [8,9]. The Faraday effect enhances the efficiency of optical fiber sensors in measuring magnetic fields, particularly in high-current applications, but it presents challenges such as measurement complexity, optical loss, and limited linearity of response [10]. Advances in optical communication technologies have significantly improved their performance. However, technical challenges remain in integrating all these improvements into a single commercial device [11]. Studies based on the Faraday model highlight the importance of exploring diverse materials to enhance the Faraday effect across different wavelengths and devices [12]. Despite progress in fiber optics fabrication and advances in such field in general, integrating essential optical elements, such as wavelength filters, partial reflectors, and mirrors with fiber optics remains a challenge [13].

However, this situation has recently changed, thanks to the ability to modify the core refractive index of single-mode optical fibers by absorbing ultraviolet light. More recently, the light sensitivity of optical fibers has enabled the fabrication of phase structures directly in the fiber core, known as Fiber Bragg grating (FBG), as shown in Figure 2 [14]. These gratings come in four types: single grating, double grating, triple grating, and quadruple grating. In each region, Bragg wavelength increases by approximately 6 nm, with the distance between each region remaining constant. The laser's reflection (R) and transmittance (T) spectra, as well as the number of its peaks and bandwidths, are monitored and analyzed at constant temperature and stress. The period of the index of refraction variation represented by a broadband light is coupled into the core of the fiber. Part of the input light is reflected (at the Bragg condition) and the rest is transmitted. The reflected and transmitted light bandwidth related to Bragg grating characteristics, which are modulation depth and Bragg grating length [15].

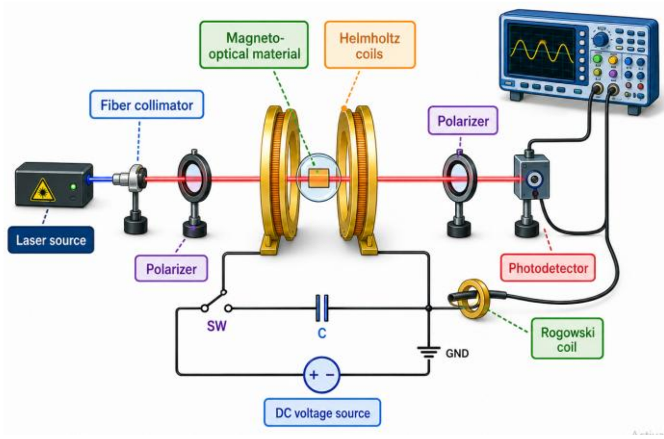


**Fig. 1.** Faraday Experiment setup.

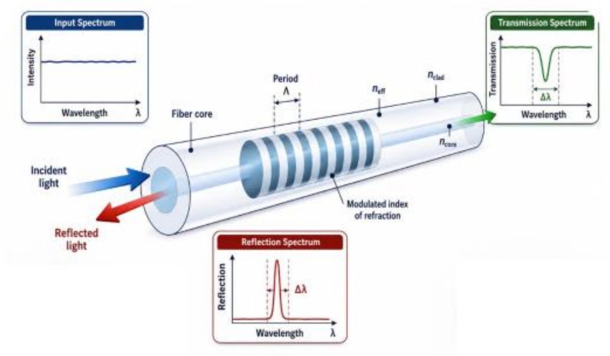


**Fig. 2.** Bragg grating inscribed into the core of an optical fiber.

### 1.2. Verdet Constant Measurements

In FBG, light is coupled between forward propagating mode to backward propagating mode, so the reflected Bragg wavelength ($\lambda_B$) is given as [16, 17]:

$$\lambda_B = 2\, n_{\text{eff}}\, \Lambda \tag{1}$$

Where, $n_{\text{eff}}$ is effective index of refraction, Λ is period of grating measured in ($nm$).

The Faraday rotation strength can be quantified with Verdet constant ($V$), this leads to deduce the rotation degree (Δφ) per magnetic field induction ($B$) unit along the length (L) of beam propagation and fiber Bragg unit [18].

$$V = \frac{\Delta\emptyset}{BL} \tag{2}$$

Or

$$\Delta\varphi = V.\,B.\,L \tag{3}$$

Where, the value of $V$ is a function of wavelength measured with thickness of several tens of micrometers, which can be written as follows:

$$\mathrm{V}(\lambda) = \frac{1}{\lambda}\,\frac{(n_o^2-1)}{2n_o}\,\left[A + \frac{B}{\lambda^2-\lambda_o^2}\right] \tag{4}$$

Where $\lambda$ is the operating wavelength, $\lambda_o$ is the resonance wavelength used in the dispersion model, $n_o$ is the refractive index of silica , and A and B are the empirical fitting coefficients The approximation coefficients giving maximal coefficient of determination in the 1.2-3 $\mu m$ region, where $A$=7.9 $\mu m{\cdot}rad/(T{\cdot}m)$, $B$=19.3 $\mu m{\cdot}rad/(T{\cdot}m)$, and $\lambda_o$=1×10$^{-3}$ $\mu m$. The dependency dispersion in refraction index $n_o(\lambda[\mu m])$=3.413+0.15/($\lambda$ [20.0042]) achieved with the help of data at room temperature [19].

### 1.3. Magnetic Field Sensitivity

From the Faraday effect, the magnetic sensitivity (S) represents the ratio of the power variation ($dP$) to the magnetic field variation ($dB$) as follows [20]:

$$S = \frac{dP}{dB} \quad (5)$$

Then, when using the polarization, Mule's law of the power is given as [21]:

$$P = P_o cos^2\varphi \quad (6)$$

Using chain rule, Eq. (5) can be written as:

$$S = \frac{dP}{d\varphi} \cdot \frac{d\varphi}{dB} \quad (7)$$

The equation (3) can be written as $\frac{d\varphi}{dB} = V\,L$, where φ is angle of rotation and $L$ is the interaction length of the light in the fiber. Differentiating from Eq. (6) with respect to the rotation angle $\varphi$, we obtain

$$\frac{dP}{d\varphi} = -\,2\,P_o \cos\varphi \sin\varphi \quad (8)$$

Substituting Eq (8) in Eq(7) to find sensitivity $S$

$$S = -2P_o \cos\varphi \sin\varphi\, VL \quad (9)$$

In mathematics, sin 2$\varphi$ = − cos $\varphi$ sin$\varphi$, then:

$$S = P_o VL \sin 2\varphi \quad (10)$$

At small angle of rotation ($\varphi$<< 1), the sin2$\varphi\simeq$2$\varphi$is applied

$$S = P_o VL\,(2\varphi) \quad (11)$$

$$S = 2\,P_o VL\,(VLB) \quad (12)$$

$$S = 2P_o BL^2V^2 \quad (13)$$

For small magnetic field, the sensitivity is given by:

$$S = \frac{dP}{dB} \quad (14)$$

## 2. Related Works and Contribution

Numerous published studies have addressed the design of magnetic field sensors using fiber optics. Some studies differ in the wavelengths of light they detect, while others focus on specific materials, sizes, and designs. The following is a brief overview of the most relevant and recent research, its findings, and our own scientific contribution.

### 2.1. Related Works

Numerous published studies utilize fiber optics in the design of various sensors, some employing Faraday principles, while others are simpler. The following are some of the most important studies addressing the design of magnetic sensors, outlining their operational methods and key findings:

Liang proposed a sensor of magnetic field consisting a series of tapered, inclined optical fibers (STTF) embedded with a magnetic fluid [22]. The compact STTF structure consisted of two closely spaced, tapered fibers approximately 836$\mu m$ in length, which improved mode coupling. The transmission characteristics of the proposed sensor were studied under different magnetic field intensities (MFI). The results showed excellent response of the proposed structure to magnetic field intensities, with a maximum sensitivity of 32.67$ppm/Ørsted$ and a transmission sensitivity of 0.0336$dB/Ørsted$ within the 0–75$Ørsted$ range. The resolution of the proposed sensor reached 0.6734$Ørsted$. This makes sensors highly useful for measurements of weak magnetic field due to its good sensing performance and compact structure [22]. Thiago in 2021 proposed sensors of optical fiber interferometry called Fiber Sensor Structures (FSSs) for measurements related to magnetic field. These approximately 100 $mm$ long, coreless fiber doped with terbium oxide ($Tb_4O_7$) used to improve the Faraday constant and enhance the modulation, and resulted optical interferometry signal. The response of each sensor was evaluated at static magnetic fields with different $Tb_4O_7$ doping concentrations of (6–10$mol\%$), resulting in a 59-fold increase in sensitivity and a 6-fold increase in resolution (1.86×10$^{-2}$$mTs$, when using 6 mol-doped fibers). These results are comparable to those achieved by more complex fiber-based sensors such as fiber interferometers. The first demonstration of multi-mode magnetic field FSS was dependent on magnetooptical glass (MO) to take advantage of both polarization mode shift and Faraday rotation [23].

Samundra 2025 refer to the important application of the optical fiber with using Zn O, LCDs, LEDs, laser diodes, photodetectors, solar cells, energy harvesting devices, transistors, sensors, catalysts, active sunscreen chemicals, and other optoelectronic devices [24]. Furthermore, depolymerization processes of the glass grid were modified to accommodate more Tb ions. This resulted in a standard effective concentration (14.19× 10$^{21}$$1/cm^3$) of Tb ions in the glass, leading to a high Verdet constant of 113radians/($Ts{\cdot}m$) at 650$nm$. The sensor achieved a sensitivity of 0.139$rad/Ts$. This contributes to the development of high-performance, thermally stable metal oxide glass fabrication. Zhihang in 2023 used AC magnetic field modulation to correlate the phase containing the DC magnetic field information with the component of fundamental frequency in interfered signal [25]. Later, the signal was demodulated using experimental pattern analysis to achieve components of fundamental frequency. This sensor showed 4.651$mV/\mu T$ sensitivity at resolution of 1.649$nm$ and magnetic field range of 0–40$mT$, indicating advantages in high stability, resistance to electromagnetic interference, and miniaturization. Jiadong in 2024 employed a reduction strategy to control the valence of terbium in glass to achieve a high magneto-optical effect [26]. Titanium dioxide ($TiO_2$), characterized by the low valence of $Ti^{2+}$ ions and good reductivity, was used to inhibit the oxidation of $Tb^{3+}$ ions to $Tb^{4+}$. In $TiO_2$-$B_2O_3$-$Al_2O_3$-$Na_2O$ glass, a 10$mol\%$ concentration of $TiO_2$ could increase the Verdet constant at 650*nm* by 19%. With increasing terbium oxide ($Tb_2O_3$) concentration, the Verdet constant reached a high value of 117 $rad/(T{\cdot}m)$ at 650*nm*, which was close to the Verdet constant of TGG crystal (121 $rad/(T{\cdot}m)$), representing a novel approach for increasing the Verdet constant in fiber optics, optical isolators, and modulators. Zhongchao in 2025 proposed a sensor of magnetic field dependent on an external Fabry-Perot interferometer (EFPI) cavity in an optical fiber, achieved by coupling a giant passive magnet (GMM) to the Fabry-Perot (FP) cavity [27]. This design employed the sensing element TbDyFe. Then, the FP cavity established by precisely aligning the surface end of a single-mode optical fiber with the smooth surface of a permanent magnet. When changing the external magnetic field, GMM rod length changed accordingly, which in turn led to vary the length of FP cavity Experimental findings indicated the sensor achieved a maximum sensitivity of 676$nm/mT$ within the range of 0 up to 150$\mu T$, corresponding to a magnetic field measurement accuracy of 147$nmT$. A temperature separation method using a FBG was proposed in their work to compensate for the effect of temperature on the sensor and correct the magnetic field measurement results, thus resolving the issue of temperature cross-sensitivity.

Zaman 2026 findings offer useful design recommendations and optimization insights for medical equipment applications and optical fiber communication systems [28]. The stability of the Verdet constant is a prerequisite for measuring electric current under radiation. The simulation included the formation of nuclear plasma (deuterium-tritium) and magnetic fusion, with radiation accumulation at doses up to megagray. The simulation results showed some changes happened in induced radiation of Verdet constant with accuracy margin of (0.56%) when using gamma rays of 770 *kilogray* dose.

### *2.2. The Aim and Contribution*

The aim is to design a new sensor of magnetic field dependent on the use of Bragg fiber in a Faraday experiment setup, instead of conventional fiber, to overcome the performance limitations. This allows for studying the effect of the number of grating regions on sensor efficiency by calculating the Verdet constant of the material used in this fiber (silica) and then comparing it with conventional fiber.

The scientific contribution includes developing Faraday's experiment to design a magnetic field sensor that is tested using a fiber-Bragg of four types: FBG1, FBG2, FBG3, and FBG4 which contain one, two, three, and four gratings respectively, in addition to using the traditional SMF type. Figure 3 demonstrates the systematic diagram of FBG at two regions.

## 3. Proposed Modified Experiment Setup

The Faraday experiment setup was adopted for the sensor design of the magnetic field. It is intended to find the sensitivity of the magnetic field by using the Faraday rotation when using FBG between two coils, in which the magnetic field caused to small shifting the wavelength of the FBG due to varying the index of refraction resulted from magneto-optical effect. The modification to the setup was in the middle section, where the empty core was replaced with a fiber optic grating, and an infrared beam was used instead of visible light. Figures 4 and 5 show respectively the schematic and a photo of the setup of the proposed modified Faraday experiment in the laboratory. This also necessitated placing a polarizer after the laser light source to polarize the beam before passing it through the Faraday coils. After the laser light passes through the fiber and the Faraday coils, which generate a magnetic field, the transmitted light is collected on the spectrometer. The electromagnet used in the experiment consists of a thin U-shaped iron core, two coils of 600 turn, and perforated polarity pieces. The electromagnet is then securely fixed to the table by a rod. After measuring the magnetic flux density distribution, one meter of single-mode fiber and a Bragg fiber mesh with a different number of mesh areas are inserted into the slots of the electrode segment. The lever is then raised in order to place the magnet in the experimental setup between the two polarizing filters.

When a certain voltage (v) is applied to the electrical circuit, a magnetic field is induced. The magnetic field causes Faraday effect that makes the polarization vector of the light to rotate toward the direction of light propagation. This induces polarization vector rotation in the light that is proportional to the Verdet constant (V) of fiber material, which is silica. Therefore, measuring the Verdet constant of optical fibers involves observing the polarization change ($\Delta\varphi$) of the signal progress through less segment of the fiber under the magnetic field.

To determine the optimal distance (d) between the hollow rectangular section and the two coils in the absence of fiber, the magnetic flux density distribution in the space of hollow rectangular section and the coils is determined. Using the axial probe of a Teslameter, which can be easily moved through one of the electrodes cutting slots when secured in a universal clamp on a sliding stand, the flux density is measured across the entire distance between the two coils in 20-35mm increments. This process is repeated for different currents (0.5-3A) resulting from adjusting the coil circuit voltage to 20–100v, changing 20v each time. Changing the voltage alters the current in the coil circuit and thus changes the magnetic flux density. The sensitivity (S) for each case in the study can then be calculated from the relationship between the power (P) measured by the perimeter and the magnetic flux density measured by the Teslameter, after adjusting the measurement units to ensure compatibility. To ensure optimal sensitivity, it was crucial to monitor the system's behavior to achieve the ideal state where no design modifications were required. The number of gratings was expected to be proportional to the system design; increasing the number of stimulators might not significantly improve sensitivity, causing it to plateau or even decrease in the presence of negative interference or energy loss. Subsequent experiments demonstrated that the optimal number of gratings for the modified Faraday experiment was four. Therefore, four types of fibre Bragg were used: FBG1, FBG2, FBG3, and FBG4, in addition to the conventional SMF type.

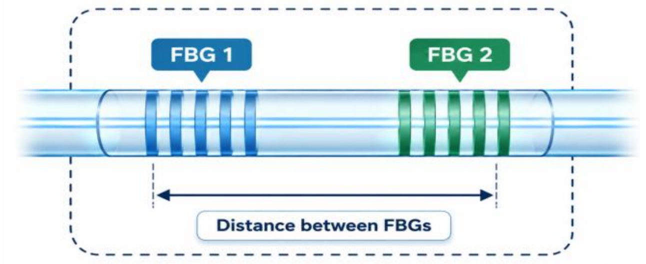


**Fig. 3.** Systematic diagram of FBG at two regions.

It was intended to use a 1*m* length of SMF fiber with four types of Bragg fibers: Type FBG1 contains one 10*mm* grating of the total 1*m* fiber length; Type FBG2 contains two 10*mm* gratings spaced 0.5 *mm* apart; Type FBG3 contains three 10*mm* gratings spaced 0.5*mm* apart; and Type FBG4 contains four 10*mm* gratings spaced 0.5*mm* apart, each of type: Acrylate SMF-28e and 1530.466-1550*nm* with 98-99.61% reflectivity, as shown Figure 3.

## 4. Results and Discussions

The density distribution of the magnetic flux in between the rectangular hollow section and coils was examined in the absence of a fiber. It was found that the flux density sharply rises in the gap's center and falls on either side. Figure 6 displays these findings; it shows the behavior of measured magnetic field (B) as a function of the distance between the two coils (d) changed from 5-35mm by step of 5mm each. From this, we can find that the best value of B is at the middle distance of 20mm for all values of currents used, which ranged from 0.5-3A (see Table 1).

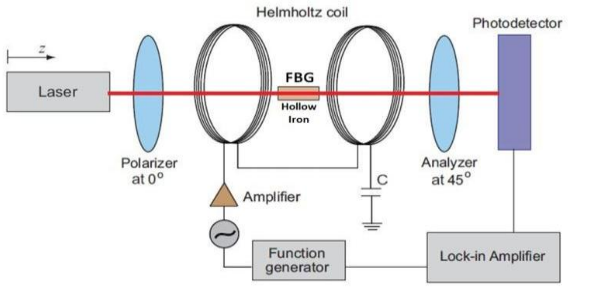


**Fig. 4.** A diagram illustrating components of modified Faraday experiment system.

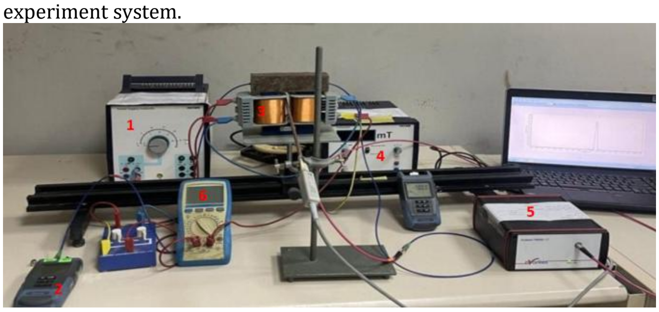

**Fig. 5.** A photo of proposed modified Faraday experiment setup in the laboratory, consisting; a power supply, a 1550nm wavelength laser, two coils of 600 turns, a Teslameter of ∓0.03*mT*, a Spectrometer Ava Space-NIR ranged 1000-1750; with laptop, and an Ameter.

**Table 1.** Values of the magnetic field (*B*) resulting from the change in distance (*d*) between the two coils in the absence of the fiber at different currents (*I*).

| d(mm) | I=0.5 A B(T) | I=1 A B(T) | I=1.5 A B(T) | I=2 A B(T) | I=2.5 A B(T) | I=3 A B(T) |
|---|---|---|---|---|---|---|
| 5 | 0.02 | 0.1 | 0.15 | 0.2 | 0.2 | 0.22 |
| 10 | 0.13 | 0.55 | 0.8 | 0.91 | 1.21 | 1.31 |
| 15 | 0.14 | 0.54 | 0.83 | 0.93 | 1.32 | 1.42 |
| 20 | 0.17 | 0.58 | 0.88 | 1 | 1.35 | 1.45 |
| 25 | 0.13 | 0.51 | 0.8 | 0.91 | 1.3 | 1.4 |
| 30 | 0.1 | 0.1 | 0.12 | 0.2 | 1.2 | 1.33 |
| 35 | 0.05 | 0.05 | 0.001 | 0.01 | 0.05 | 0.07 |

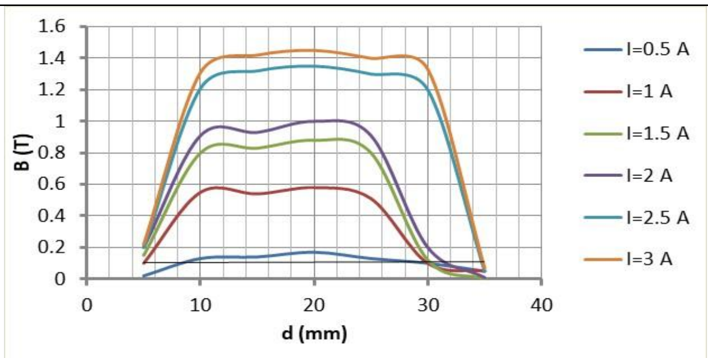


**Fig. 6.** Magnetic flux density between the two coils with different d at different I.

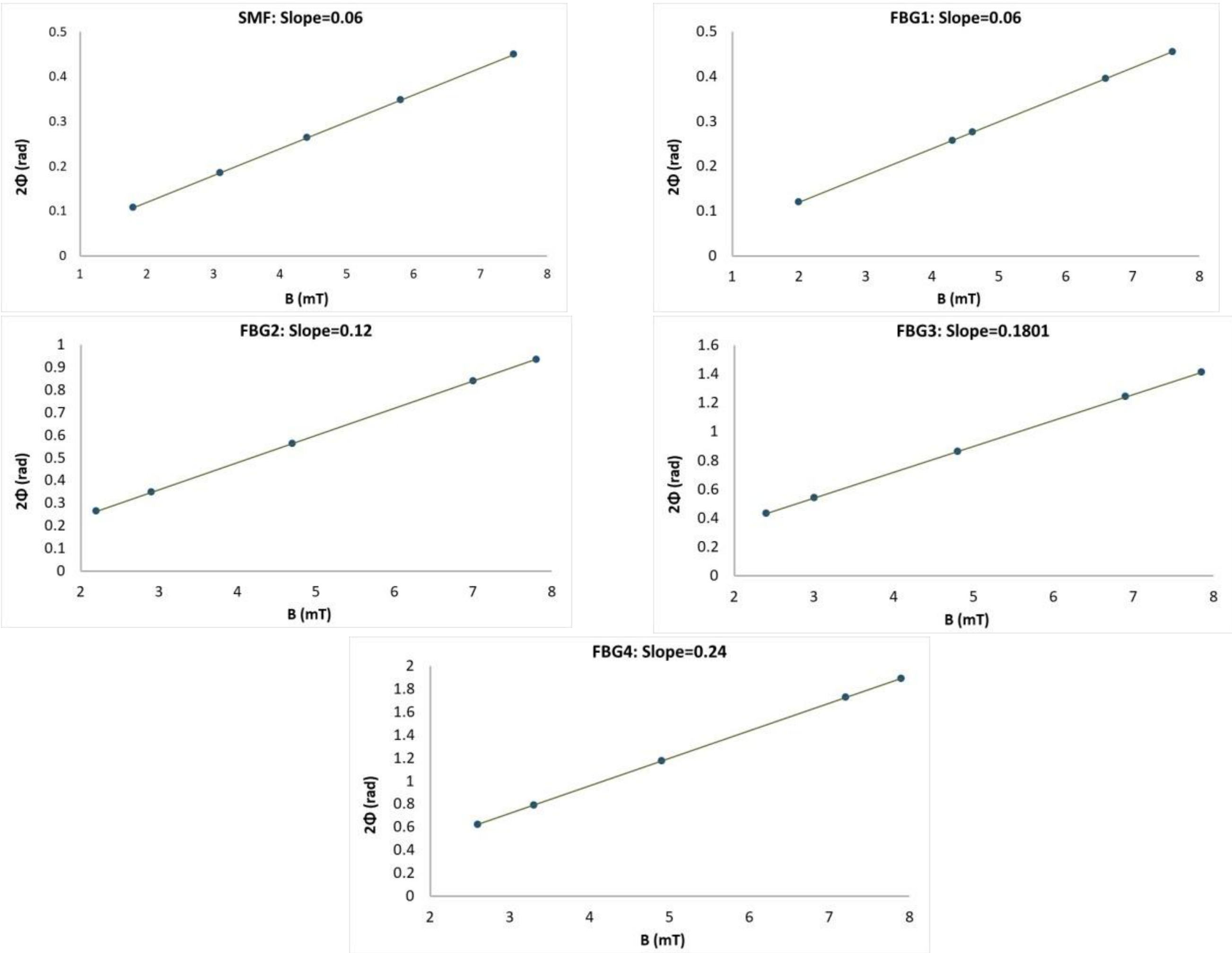


**Fig.7.** Angle of rotation (2φ) variation with changes in the magnetic field flux (B) for all types of fibers used.

**Table 2.** Measured Verdet constant using slope of Figure 7.

| Fiber Type | Slope=2φ/B | L($mm$) | V ($rad/T.m$) |
|---|---|---|---|
| FBG1 | 0.06 | 10 | 3 |
| FBG 2 | 0.12 | 20 | 3 |
| FBG 3 | 0.1801 | 30 | 3.001 |
| FBG 4 | 0.24 | 40 | 3 |

In this Figure, the largest measured value of the magnetic flux in the gap between two electro-magnetic poles can be used to estimate the average magnetic flux density of the tested sample at a constant coil current. The use of electromagnets to generate the magnetic field in this experiment was useful in determining the relationship between the average magnetic field in the vacuum between the poles and the current applied to the electromagnets using the curve-fitting method. A linear curve of the average magnetic field as a function of the applied current was fitted, as shown in Figure 6.

The relationship between the angle of rotation (2φ) and the current applied to electromagnets can also be observed to illustrate the degree of rotation of the polarized beam relative to the change in magnetic field strength. Figure 7 shows the change in angle 2φ with the change in the average magnetic field when using a wavelength of 1550 *nm*. The equation that governs the relationship between angle 2φ as a function of the average magnetic field at a wavelength of 1550 nm is $2\varphi = V \times B \times 2L$ that derived from Eq.(3)

After plotting this relationship, the Verdet constant can be determined to be equal to the quotient of the slope of the best straight line divided by twice the length, 2L. Experimentally, the Verdet constant for silica has been found to be 3.1$radians/tesla{\cdot}m$ at a wavelength of 1550 $nm$. While the Verdet constant can be calculated theoretically from Equation (4), it is an experimental representation that illustrates the relationship between the angle and the length of the fiber used. It is observed that the slope of the 2φ angle behavior with respect to changing the magnetic field varies depending on the type of fiber used. Referring to equation (3), we find that this variation depends on the Verdet constant multiplied by the length of fiber bar for all types of fibers used in the experiment, as shown in the Table 2.

Figs. 8 represent the variations of the magnetic field as a function of current. It is noted that the magnetic field varies linearly with current, and the magnitude of the sensitivity also increases with the number of gratings regions. This indicates that the generated magnetic field values were greater in the FGB type fiber than in the SMF type. It can be observed that this increase is highest in the FBG4 type fiber because the increased number of gratings within the fiber means that light passes through more interaction regions, thus increasing the Faraday effect and consequently leading to an increase in the magnetic flux. This magnetic field produced due to BαI in the optical fiber causes a polarization change or phase change for the light in the presence of the gratings, as each grating acts as a sensing point.

As a result, the magnitude of the change in the optical signal increases, as clearly shown in Figure 8. Furthermore, it was found that increasing the number of gratings leads to increase the effective length, then consequently, an increase in the value of φ, i.e., a higher polarization of the light is achieved.

Fig.s 9 illustrate the relationship between power (P) and the magnetic field, which appears as a linear increasing relationship. The slope represents the sensitivity value for each type of fiber used. It is observed that the slope of the best straight line for the relationship between power and magnetic field for the SMF type fiber, representing the average percentage of sensitivity, is a good value of 69.382 w/T. However, average sensitivity percentage decreases in the FBG1 type fiber to 65.867 w/T, then increases again in the FBG2, FBG3, and FBG4 types to 71.824 w/T, 73.819 w/T, and 74.628 w/T respectively, as shown in Figure 10. This figure also shows that the highest values are found in type of used fiber at higher applied voltage of 100v, in which the highest sensitivity percentage calculated for FBG4 is 93 w/T at a magnetic field of 7.9$mT$ and a voltage of 100$v$ as given in Table 3. Table 4 presents only the highest values of the sensitivity for each type of used fibers, which is represented in Figure 10 too, where the voltage (Vi) is set within the specified range 20-100$v$, and the current (I) is measured using an Ammeter to compute the power ($P=VI$), while the magnetic field flux (B) is measured using a Teslameter.

It is shown that increasing the number of gratings increases the effective length and the angle, leading to an increase in sensitivity, reaching its highest value in the FBG4 type. The reason this type of grating exhibits the highest sensitivity is due to three factors: the occurrence of a maximum effective length, the accumulation of the Faraday effect across multiple regions, and the enhancement of interference/reflection acting as a selective mirror for the FBG. Reaching this value of 74.628 w/T may be the optimal limit, because beyond this value, saturation occurs, and the angle becomes too large, causing light loss and signal distortion due to multiple reflections. Furthermore, any increase in the number of gratings beyond four will not continue to increase the sensitivity but will instead lead to a decrease.

The difference in sensitivity values with different fiber types is due to the way light interferes within the fiber. With multiple grating, small changes in the magnetic field are amplified, increasing detection sensitivity. Each additional grating enhances the overall effect, making the device more capable of detecting small changes. Multiple grating amplifies the signal further, thus increasing sensitivity.

Conversely, a single grating may not be sufficient to detect subtle changes. A single grating is weak in amplifying interference or effect. In other words, the sensing power depends on amplifying changes. With a weak grating, the effect is less pronounced, making it difficult for the system to detect small changes.

The reason SMF fibers are more sensitive than FBG1 fibers is that single-mode SMF fibers are designed to minimize internal noise and maintain a single light pattern. This results in a more stable response and is less affected by noise. With a single-mode fiber, the effect can be less pronounced because the design does not utilize the same balanced interference pattern. Therefore, single-mode fibers sometimes provide a stronger response, despite their simplicity.

Fig. 11 represents the spectra of light counts vs wavelengths used for different types of fibers used, and the number of peaks in each behavior indicates the presence of the number of gratings in each fiber. No significant wavelength shift or peak broadening is observed in the spectra. This indicates that the applied magnetic field does not induce a measurable change in the effective refractive index of the fiber.

Therefore, the magnetic response is dominated by polarization rotation rather than spectral displacement, consistent with a weak magneto-optic response of standard silica fibers. At the operating wavelength of 1550$nm$, the Verdet constant is relatively small compared to its value in the visible region. This explains the absence of noticeable spectral changes and highlights the need for either stronger magnetic fields or magneto-optic materials to enhance sensitivity in the near-infrared regime. In SMF, one can conclude that the narrow and stable spectral peak at 1550$nm$ provides a reliable platform for measuring Faraday-induced polarization rotation, this is due to the total internal reflections of light inside the fiber. In correspondence, the spectral behavior of remaining FBG types is observed to contain more than one peak due to the simultaneous presence of both transmission and reflection, and the number of these peaks increases with the number of gratings regions in the fiber. In the third and fourth cases, the third and fourth peaks may be indistinguishable due to their small size and close proximity that appeared wide spectral peak at 1550$nm$.

However, the lack of observable wavelength shift confirms that the Verdet constant of the employed fiber material is low, which is consistent with the weak magneto-optic response of silica in the near-infrared region. Also, under a magnetic field, Faraday induced polarization rotation can redistribute optical power between polarization states. If the detection system is polarization-sensitive, this may lead to apparent intensity enhancement or saturation without a clear wavelength shift.

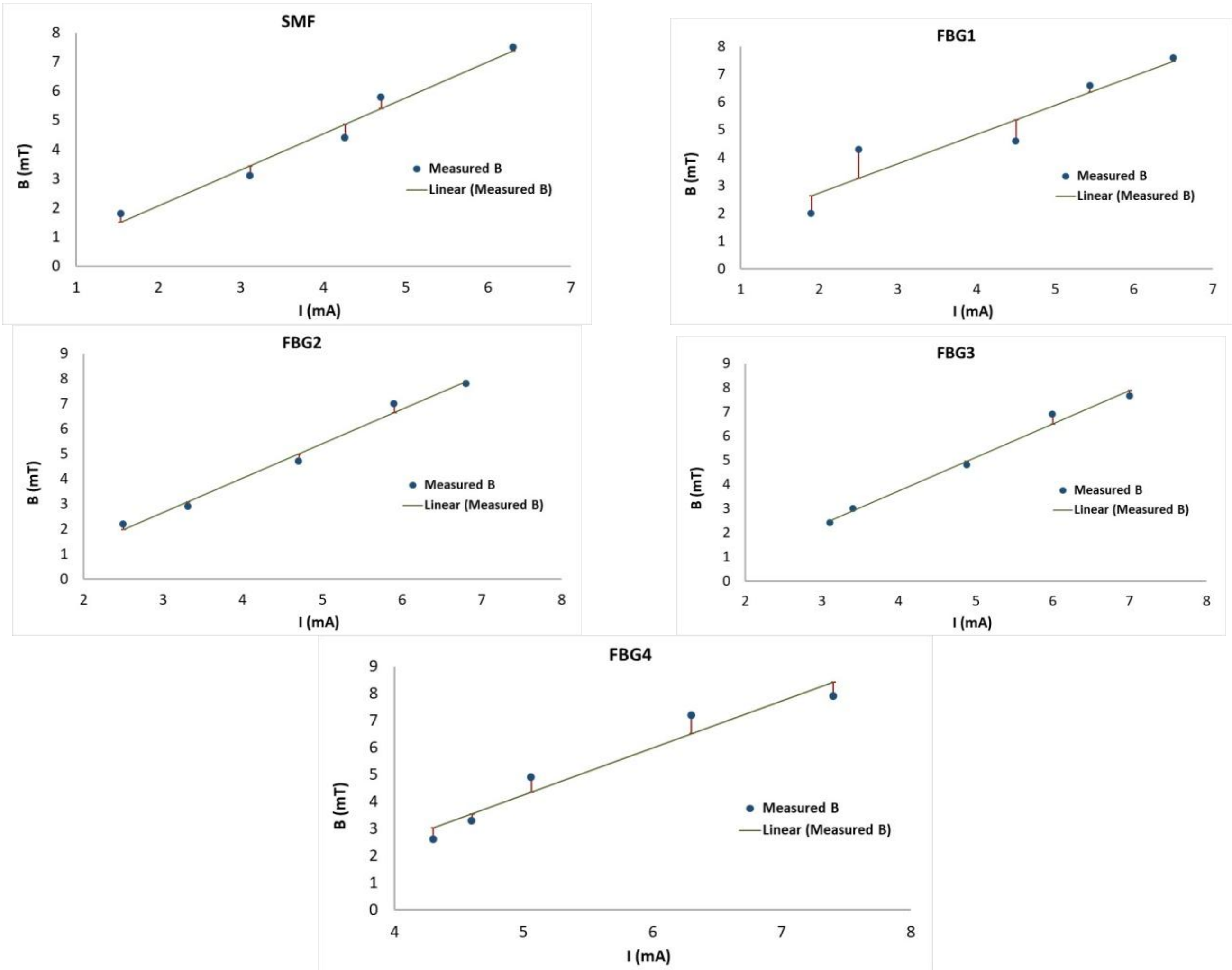


**Fig. 8.** The magnetic field vs current for all types of fibers used.

**Table 3.** Experimental values obtained for FBG4.

| **Vi (*v*)** | **I(mA)** | **P(mw)** | **B(mT)** | **S** (w/T) |
|---|---|---|---|---|
| 20 | 4.3 | 86 | 2.6 | 30.07 |
| 40 | 4.6 | 184 | 3.3 | 55.70 |
| 60 | 5.06 | 303.6 | 4.9 | 62.00 |
| 80 | 6.3 | 504 | 7.2 | 70.00 |
| 100 | 7.4 | 720 | 7.9 | 93.00 |

**Table 4.** Parameters' values of highest sensitivity (Vi=100*v*).

| **Fiber** | **I(mA)** | **P(mw)** | **B(mT)** | **S** (w/T) |
|---|---|---|---|---|
| SMF | 6.3 | 630 | 7.5 | 84 |
| FBG1 | 6.5 | 650 | 7.6 | 85 |
| FBG 2 | 6.8 | 680 | 7.8 | 87 |
| FBG 3 | 7 | 700 | 7.85 | 89 |
| FBG 4 | 7.4 | 720 | 7.9 | 93 |

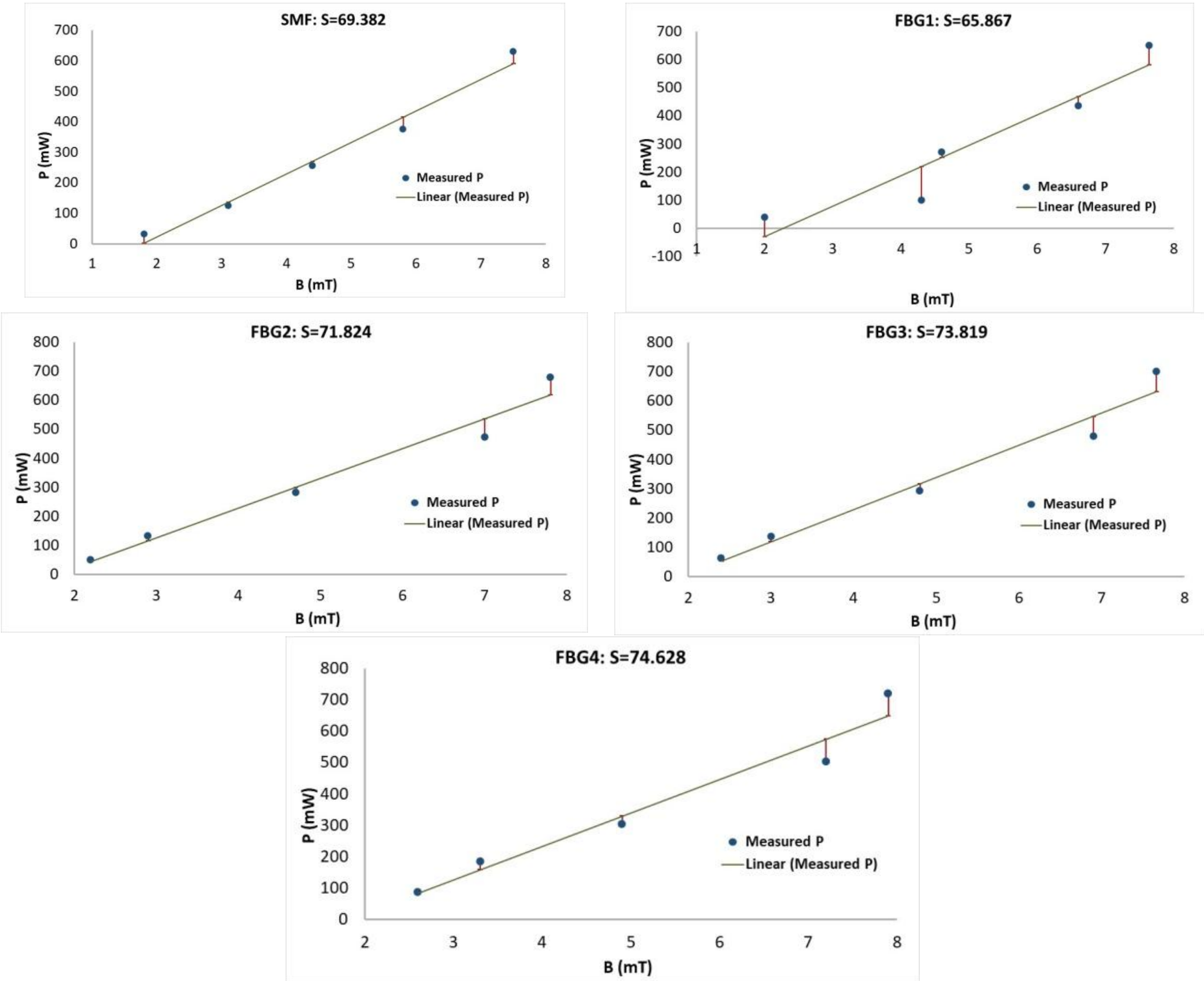


**Fig. 9.** The variation of Power (P) as a function of magnetic field (B).

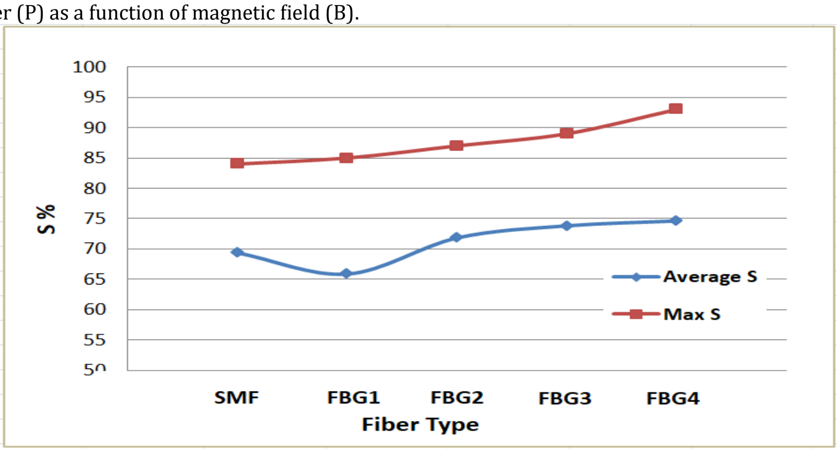


**Fig. 10.** The maximum and average values of the sensitivity for each type of fiber used.

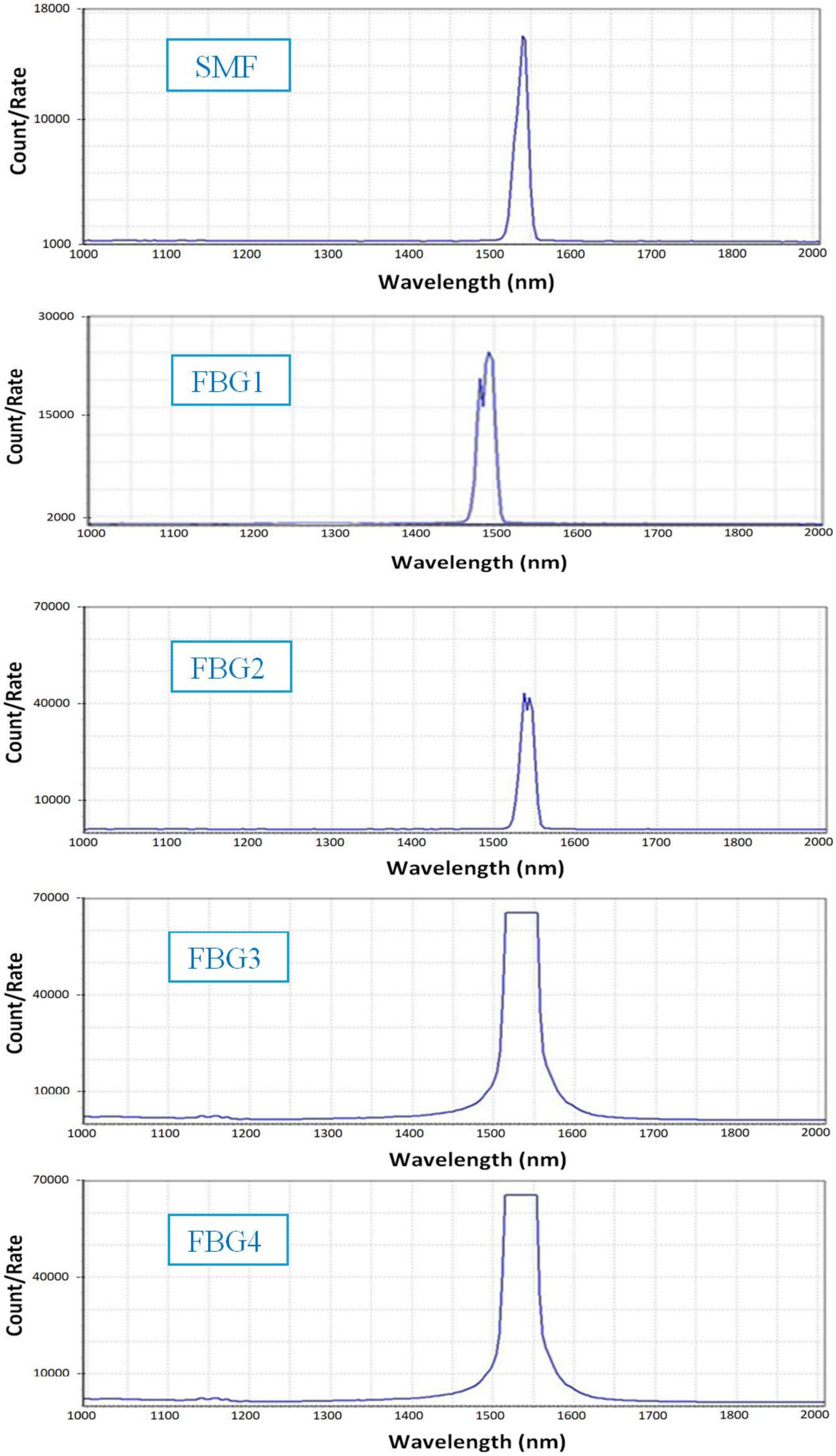


**Fig. 11.** The spectrum behavior of the used SMF and Bragg fibers with wavelength.

## 5. Conclusions

This research investigated the effect of magnetic fields on the propagation characteristics of light within optical fibers, based on the Faraday effect. The focus was on determining the Verdet constant and analyzing the optical fiber's response to various magnetic variations. The results showed that increasing the magnetic field strength led to a significant change in the polarization rotation angle and the spectral characteristics of the optical signal, confirming the efficiency of optical fibers as sensitive elements in magnetosensing applications. We also found that using Bragg structures or multi-zone structures improved sensitivity and resulted in higher measured accuracy compared to conventional fibers. This is due to enhanced interaction between the magnetic field and the light wave within the optical fiber. The results obtained were well consistent with theoretical principles and previously published studies, supporting the validity of the proposed model and the efficiency of its design.

## Acknowledgments

I extend my sincere thanks and appreciation to everyone who contributed to the completion of this research, and I especially thank my fellow researchers for their scientific support, valuable guidance, and continuous follow-up throughout the research process. I also express my gratitude to the colleagues and friends who helped provide the necessary feedback and scientific resources.

## Funding Statement

This research received no specific grant from any funding agency.

## Conflicts of Interest

The authors declare that they have no known competing financial interests or personal relationships that could have appeared to influence the work reported in this paper.

## Authors' Contribution Statement

All authors contributed equally to this work.

## References

[1] Tiwari, N., Mishra, U., Kaler, R.S., Jain, S.C., Singh, N. and Kapur, P., 2012. Fiber Bragg grating based technique for sensing current. *Experimental Techniques*, 39(4), pp.9-12.

[2] Tan, C.Z. and Arndt, J., 1997. Faraday effect in silica glasses. *Physica B: Condensed Matter*, 233, pp.1-7.

[3] Madhav, K.V., Ravi Kumar, K., Srinivas, T. and Asokan, S., 2006. Fiber Bragg grating magnetic field sensor. In *Proceedings of the IEEE Instrumentation and Measurement Technology Conference (IMTC 2006)*, Sorrento, Italy, 24–27 April 2006, pp.2042-2044.

[4] Ismaeel, R., Masoudi, A., Wang, Y., Talataisong, W. et al., n.d. Giant Faraday rotation in gadolinium-doped silica optical fibers for high-performance optical isolators. Available at: http://www.osapublishing.org/submit/ocis/ (Accessed: 14 July 2026).

[5] Song, N., Wang, X., Xu, X., Cai, W. and Wu, C., 2017. Measurement of the Verdet constant of polarization-maintaining air-core photonic bandgap fiber. *Sensors*, 17(8), Article 1899.

[6] Chen, J., Huang, S.-Y., Lin, C.-Y. and Liu, W.-F., 2022. A low-frequency magnetic field sensor based on fiber Bragg gratings. *Photonics*, 9(2), Article 102.

[7] Hill, K.O. and Meltz, G., 1997. Fiber Bragg grating technology fundamentals and overview. *Journal of Lightwave Technology*, 15(8), pp.1263-1276.

[8] Alhussein, A.N.D., Qaid, M.R.T.M., Agliullin, T. et al., 2025. Fiber Bragg grating sensors: Design, applications, and comparison with other sensing technologies. *Sensors*, 25, Article 2289.

[9] Mihailovic, P. and Petricevic, S., 2021. Fiber optic sensors based on the Faraday effect. *Sensors*, 21, Article 6564.

[10] Rostami, A., Wahaab, F.A., Soleimani, H. et al., 2023. Advances in fiber Bragg grating technology for magnetic field sensing: A review. *Measurement*, 221, Article 113482.

[11] Zheng, J., Dong, X., Zu, P., Shao, L.-Y. et al., 2013. Magnetic field sensor using tilted fiber grating interacting with magnetic fluid. *Optics Express*, 21(15), pp.17863-17868.

[12] Liu, Z., Chen, Z., Chen, N.A. et al., 2020. Study of the Verdet constant of the holmium-doped silica fiber. *OSA Continuum*, 3(5), pp.1096-1104.

[13] Descamps, F., Kinet, D., Bette, S. and Caucheteur, C., 2016. Magnetic field sensing using standard uniform FBGs. *Optics Express*, 24(23), pp.26152-26160.

[14] Snetkov, I. and Yakovlev, A., 2022. Faraday isolator based on crystalline silicon (c-Si) for 2 μm laser radiation. *Optics Letters*, 47, pp.1895-1898.

[15] Othonos, A., Kalli, K., Pureur, D. and Mugnier, A., 2006. Fibre Bragg gratings. In *Springer Series in Optical Sciences*. Berlin: Springer.

[16] Agarwal, S. and Mishra, V., 2014. Characterization of fiber Bragg grating for maximum reflectivity based on modulation depth of refractive index. *Optik*, 125(18), pp.5192-5195.

[17] Marignetti, F., De Santis, E. et al., 2016. Fiber Bragg grating sensor for electric field measurement in the end windings of high-voltage electric machines. *IEEE Transactions on Industrial Electronics*, 63(5), pp.2796-2802.

[18] Feng, D., Kai, G., Ding, L. et al., 2000. Experimental study on fiber Bragg grating electric current sensor. *Defense Technical Information Center Compilation Part Notice*, ADP011248.

[19] Bondarenko, E., Demin, M. and Morozova, T., 2025. Enhancing current sensor sensitivity using Faraday effect with multiple reflections in magneto-optical crystals. *EPJ Web of Conferences*, 318, Article 05007.

[20] Daggar, P. and Verma, S.S., 2019. Verifying Faraday's magneto-optical effect for some materials. *European Journal of Biophysics*, 7(1), pp.8-14.

[21] Barybin, S.N., Grigorenko, A.N., Konov, V.I. and Nikitin, P.I., 1991. Magnetic field fibre-optical sensors based on Faraday effect. *Sensors and Actuators A: Physical*, 27(1–3), pp.767-774.

[22] Lu, L., Miao, Y., Zhang, H. et al., 2020. Magnetic sensor based on serial-tilted-tapered optical fiber for weak magnetic field measurement. *Applied Optics*, 59(9), pp.2791-2796.

[23] Thiago, D., Douglas, F., Eric, F. and Cristiano, M., 2023. Magnetic field fiber specklegram sensors based on $Tb^{3+}$-doped magneto-optical glasses with high Verdet constants. *IEEE Sensors Journal*, 23(7), pp.6872-6879.

[24] Samundra, M., Sumitra, P., Rishi, G., Pramod, S., 2025. Effect of Aluminum Doping on the Optical, Electrical, and Gas Sensing Properties of ZnO Thin Films. *Progress in Physics of Applied Materials, 5* ,pp. 1 – 9.

[25] Zhang, Z., Cui, L., Jianhua, Y. and Shuangliang, C., 2023. Sagnac magnetic field sensor based on sinusoidal modulation and empirical mode decomposition. *Journal of Lightwave Technology*, 99, pp.1-6.

[26] Li, J., Zhang, X., Chen, Y. and Yinsheng., 2024. High Verdet constant of $Tb_2O_3$-doped TiO-$B_2O_3$-$Al_2O_3$-$Na_2O$ magneto-optical glass. *Optics Express*, 32(9), pp.16506-16513.

[27] Q., Z., Z., R., L., X. and T., Y., 2025. Optical fiber EFPI cavity magnetic field sensor based on the magnetostrictive effect. *IEEE Sensors Journal*, 99, pp.11-17.

[28] Zaman ,H.K. 2026. Numerical Analysis of Pulse Propagation in Optical Fibers Using Paraxial Wave Equations' *Progress in Physics of Applied Materials, 6* , Serial Number 13,pp. 293-303.

[29] Suryandi, A.A., NurSarma and Mohammed, A., 2022. Fiber optic fiber Bragg grating sensing for monitoring and testing of electric machinery: Current state of the art and outlook. *Machines*, 10, Article 1103.